# Extended vertical range roughness measurements in non-ideal environments

Katherine Creath*
4D Technology Corporation, Tucson AZ 85706,
Optineering, Tucson, AZ USA 85719, and
College of Optical Sciences, The University of Arizona, Tucson, AZ USA 85721

## ABSTRACT

This paper describes recent research into developing an extended range dynamic interferometry technique where the range is extended vertically to enhance surface roughness measurements made in non-ideal environments. Utilizing short pulses from two sources on either side of a frame transfer in a CCD sensor, data can be taken fast enough in noisy shop environments to make measurements in the presence of vibration, and air turbulence. A key application of this technique is monitoring of surface roughness of large optics during the polishing process by making in situ measurements from fine grind through to the final polish. It is anticipated that this monitoring can help speed up what is now a very lengthy process. This same technique is applicable to many other types of measurements including MEMS devices, as it is not affected by dispersion in windows covering devices, and for measuring features on flat panel display glass or semiconductor wafers. This paper describes the technique, and presents results of a variety of sample measurements including: bare glass in various states of polish from fine grind to final polish, scratches and pits in a roughened semiconductor wafer, a DMD MEMS device, and various calibration standards. Performance in terms of repeatabilitity of step heights and roughness for this proof of concept is in the +/-2% range.

**Keywords:** phase imaging, polarization interferometry, interference microscopy, surface finish, surface roughness, optical metrology

## 1. INTRODUCTION

Microscopic surface roughness is critical to the performance of precision optical devices and equipment. If not properly controlled it can lead to losses from scattered light and blurring in the imaging system. Optical designers are increasingly placing more stringent specifications on these parameters in large optical systems. The challenge has been that commercially-available systems are limited to measuring surfaces of less than about 250mm in diameter and to measurements in vibration-isolated environments.

Current, state-of-the-art, interference microscopes for surface roughness measurement are based upon scanning techniques (white light, vertical scanning [1-3]) or temporal phase shifting interferometry [1, 3] and have been around since the early 1980's.[4-6] The problem with these systems is that because several video frames of data are taken sequentially to obtain a single phase measurement, it can take up to several seconds to acquire enough frames of interference information to determine surface topography. During the entire acquisition time these systems require vibration isolation to keep everything still over the course of a single measurement. Any vibration between the test surface and the microscope will compromise the measurement since vibration amplitude often exceeds the scale of the surface feature being measured. The required equipment to isolate this vibration is prohibitively expensive in most modern manufacturing environments.

Most interferometric microscopes have utilized narrowband illumination with short coherence lengths of tens of microns. The reason for narrowband "low coherence" illumination is to reduce effects of reflections off of nearby surfaces and to help reduce effects of speckle in the imaging systems. With dispersive samples like

* email: kcreath@ieee.org

measuring through a window of a MEMS device, low coherence illumination enables the samples to be isolated in space without getting spurious interference patterns from other surfaces (mainly the window). Dispersive samples have another problem related to coherence. The spatial coherence length needs to be small enough to isolate the surface of interest while the temporal coherence length needs to be large enough to accommodate the expected dispersion.[7, 8] In a microscope this is done both by controlling the temporal coherence of the sources and the size of the source (or aperture stop) in the entrance pupil of the microscope objective.

To dynamically acquire phase data, pixelated phase mask sensor technology uniquely provides a single frame phase measurement in a compact, robust format that is compatible with conventional microscope imagining systems, and permits the use of a wide variety of wavelengths and source bandwidths.[9-11] It enables the creation of a versatile and compact microscope interferometer for a variety of applications. These sensors have been implemented in many different types of interferometers and are insensitive to vibration and do not require scanning. All necessary information to determine phase is recorded in a single snapshot.[9-11]

Another piece that this work addresses is the need to vertically extend the range of dynamic interferometric profiling so that surfaces with roughness or dimensions greater than a quarter of the measurement wavelength may be measured dynamically in a shop environment. This requires taking the data very quickly, and having the flexibility of utilizing different source wavelength contributions.

This paper describes a novel microscope system utilizing these concepts for the primary purpose of being able to make in-situ measurements of surface roughness during the polishing process of large optics directly in the shop environment as well as for measurement of dynamically moving devices such as MEMS with windows that have dispersive properties.

## 2. BACKGROUND

### 2.1 Breadboard Linnik interference microscope

A schematic and photo of the breadboard microscope system are shown in Figure 1. An unpolarized extended source is provided through a large core multimode fiber. A polarizer in the Kohler illumination system is oriented to maximize fringe contrast by varying the amount of light going to the reference and test arms of the Linnik. The polarizing beamsplitter in the Linnik separates two linear orthogonal polarizations. The imaging system is a 1X Nikon tube lens that is broadband, but not optimized for this particular optical system. The quarterwave plate (QWP) in front of the camera converts the two orthogonal linear polarizations into right-hand and left-hand circular orthogonal polarizations that are incident upon the pixelated phase mask, which encodes the fringes into 4 different relative phase values.

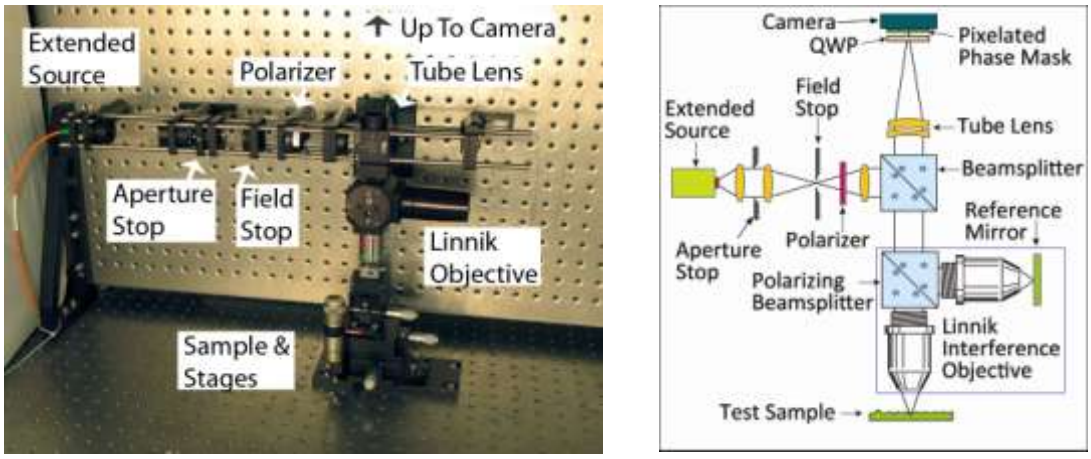


Figure 1. Layout of interference microscope breadboard with Linnik interference objective.

The main consideration for the sources used in this breadboard is coherence length. The problem with an LED source is that the coherence length is too short to be able to get high quality fringes when looking through the window of a MEMS device. To provide a versatile system, the temporal coherence length of the source needs to

be 200-300 µm so that it is long enough to accommodate the dispersion obtained when imaging through a window, yet short enough that extra sets of interference fringes are not produced from surfaces near the one being measured. [7, 8] The physical size of the source as imaged into the entrance pupil of the microscope objective will determine the spatial coherence of the microscope and limit the extent of surface structure that can be measured and provides spatial coherences of about 30-50 µm.

Another design consideration was choosing source wavelengths enabling roughness measurements of fine ground bare glass surfaces. For this proof of concept we chose an equivalent wavelength near 4 µm produced from diode laser sources with wavelengths near 660 nm and between 780-800 nm. The source module with coaligned lasers is shown in Figure 2.

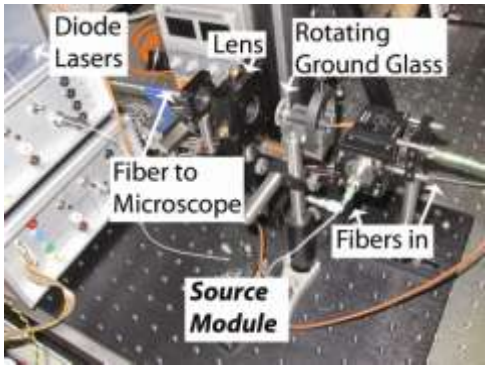


Figure 2. Multiple wavelength source module for breadboard microscope.

The pixelated phase mask is a wire grid polarizer array comprised of cells of 2x2 pixels with 4 different orientations of the individual polarizers as shown in Figure 3. Each cell of 4 pixels combines the orthogonally circularly polarized test and reference beams to produce interferogram data at adjacent pixels with relative phase shifts of 0°, 90°, 180° and 270°. The measured irradiance at each pixel of the mask is given by [12] $I(x,y) = \frac{1}{2}\left\{ I_r + I_s + 2\sqrt{I_r I_s}\cos\left[ \mathrm{D}j\,(x,y) + 2a_p \right]\right\}$, where $\alpha_p$ is the angle of the polarizer with respect to the *x, y* plane, $I_r$ and $I_S$ are the irradiances of reference and signal beams respectively, and $\Delta\phi(x,y)$ is the optical path difference between the beams. A single full field interferogram image uses all pixels of one type (e.g. A). Optical phase values are obtained by combining all 4 pixels to solve for $\Delta\phi(x,y)$ where $\lambda$ is the wavelength. There are many different solutions to this set of equations. One simple solution to obtain phase is given by $j\,(x,y) = ATAN\left\{ \frac{C(x,y) - A(x,y)}{D(x,y) - B(x,y)} \right\}$ [13]. Once phase data are obtained, the $2\pi$ ambiguities are removed using a phase unwrapped routine, [14] and then height values can be obtained by scaling by the wavelength/$2\pi$.

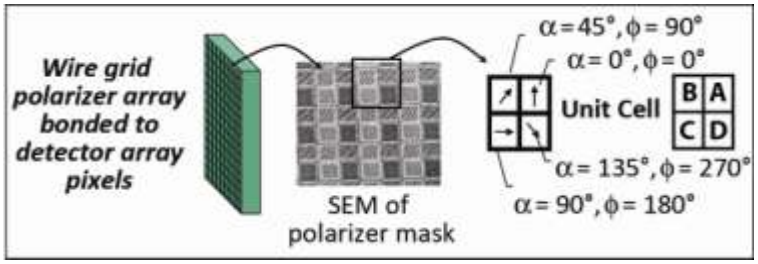


Figure 3. Pixelated phase mask and polarization orientation to determine phase.

### 2.2 Extended range multiple wavelength technique

For a multiple wavelength technique to work in optical shop and manufacturing environments, data needs to be taken quickly enough that they are not affected by vibration, noise and air turbulence. 4D Technology's pixelated phase mask technology enables taking all the data necessary to determine phase in one short snapshot. We studied various ways of obtaining two-wavelength data and determined that the best way to incorporate this with our dynamic phase measurement was to take data at two individual wavelengths in two consecutive frames from a CCD camera. With a higher speed camera, this could be scaled up to use more wavelengths if needed.

To implement this, either the camera could be shuttered, or the sources could be pulsed to obtain short exposure times. By pulsing the sources, it is easier to accommodate sources of slightly different power outputs and variations of detector responsivity with wavelength. In LabView, software was written to pulse the first source at the end of one camera frame, and the second source at the beginning of the next camera frame. The Illunis MMV-1010 camera used for this project is capable of 30 frames per second, so by adjusting the timing in this way we can take all necessary data within about 5 ms for highly reflective surfaces, and about 20 ms for bare glass surfaces. With high enough power sources, total acquisition time could easily be less than a couple hundred microseconds.

To determine phase at the equivalent wavelength, the data from the two wavelengths are combined. This can either be done directly from the irradiance data or using the calculated phase data. Determining the equivalent wavelength phase $f_e$ and the equivalent wavelength $l_e$ from the calculated phase values is simply done by subtracting the phases obtained at the two individual wavelengths [6] $f_e = f_1 - f_2 = 2pOPD\left(\frac{l_2 - l_1}{l_1 l_2}\right) = \frac{2pOPD}{l_e}$, where $l_e = \frac{l_1 l_2}{l_2 - l_1}$, and $f_1$ and $f_2$ are phases at wavelengths $\lambda_1$ and $\lambda_2$ ($\lambda_2 > \lambda_1$). Once the difference is obtained, $f_e$ is then unwrapped using standard techniques assuming there are no discontinuities larger than $l_e / 4$.

Wavelength calibration was performed using a VLSI Step Height Standard certified to be 44.1 nm high with an uncertainty of +/- 0.9 nm. This step measured 44.4 nm with 660 nm source, which is well within the calibrated range. The step measured 36.6 nm with the other source, which yields a calculated wavelength of 795 nm and an equivalent wavelength of 3.887 µm.

Although the laser diodes were equipped with TEC's (thermo-electric coolers), the wavelengths were observed to drift over time. Wavelength drift was determined by tilting a highly reflective mirror to obtain between 4-6 tilt fringes. Measurements were made over a period of time while the AC cycled and the room temperature changed by about 10°F. The peak-to-valley (P-V) measurement of the tilt was recorded to determine variations over time. This test was performed at both source wavelengths. Taking into account a single measurement instrument noise floor of approximately 1% P-V, the 660 nm source varied by +/-2 nm and the 795 source by +/-6 nm. When these errors are combined via RSS (root sum of squares), the equivalent wavelength uncertainty is about 3.1% yielding 3.887 µm +/- 0.12 µm. For better precision and repeatability, in future R&D, we will directly measure wavelength at time of measurement.

## 3. RESULTS

To present the results of our roughness measurements, the metrics used are Sa – the surface area roughness – which is the arithmetic mean deviation over the entire surface area, Ra – the arithmetic mean roughness for a single linear profile, Sq – the rms surface roughness, and Sz – the peak-to-valley (P-V) over the entire surface. Roughness standards typically are quoted in Sa or Ra. These terms are described in ISO 25178. [15, 16]

The measurements for this project were made in a lab environment that was fairly noisy. Noise sources included fans on power supplies, a HEPA filter, AC (air conditioning), and a rotating ground glass on the table next to the microscope. The temperature in the room regularly fluctuated by as much as 10°F over a 20-30 minute period. Being located under an AC vent, air turbulence caused the fringes to move substantially, precluding measurement with convention interference based profilometers. Covering the system with a plastic sheet helped reduce the movement to facilitate comparison under quiet environmental conditions. While watching the fringes

on a monitor, under the best conditions, they moved about 1/20 of a fringe frame to frame. When the fans and AC were on they moved about 1/10-1/8 of a fringe and jumped more erratically, and when the HEPA filter a few feet away was running there were regular jumps a few times a second of 1/4 of a fringe. In all these cases there was no noticeable blur from this vibration with 3 ms exposures. In a nice calm environment on a floating table with all air paths enclosed there is very little fringe motion. Because we wanted to evaluate performance in a shop environment, these noises would all be typically present.

We found we had no problem getting both frames for the multiple wavelength measurement quickly and processing them. However, we found that the chromatic aberration of the imaging system slightly shifted focus about 1-2 µm between wavelengths. Because the measurement outcome depended directly upon being in focus for each wavelength, the focus was manually verified and adjusted if needed between measurements at each wavelength for the examples we show here. In future research we intend to design a custom tube lens to correct the chromatic aberration for the chosen wavelength range.

### 3.1 Instrument noise

The noise floor of the instrument was determined by measuring a supersmooth silicon carbide mirror. When measured on commercial optical profilers under ideal conditions with extensive averaging, this surface is specified to have a roughness less than 0.1 nm. A single measurement of this mirror is shown in Figure 4 (left). The roughness is 1.194 nm Sa with an Sz of 9.96 nm.

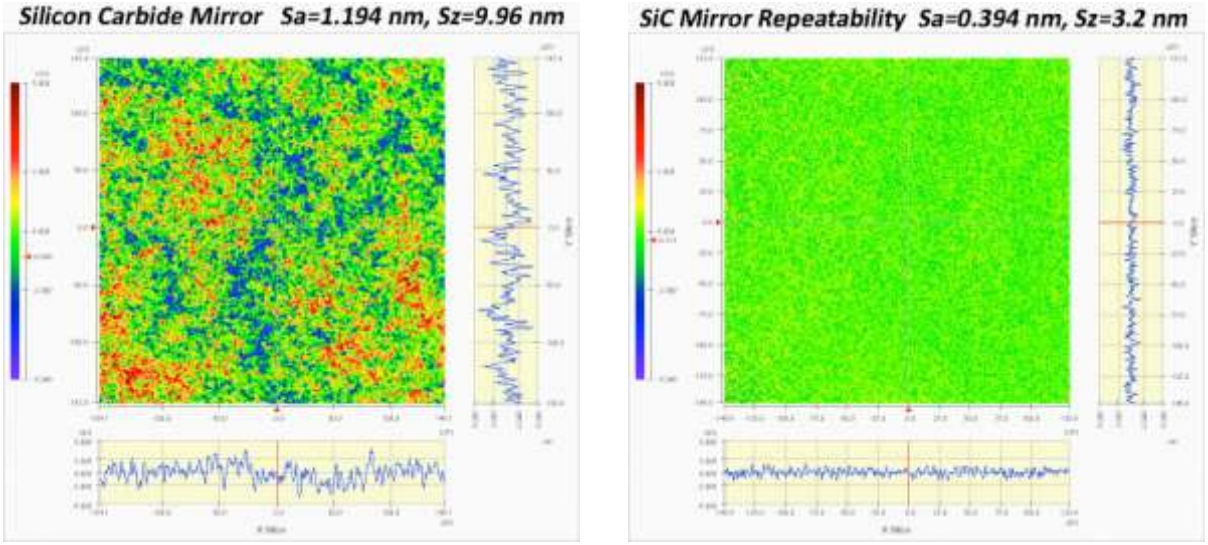


Figure 4. (left) Single measurement of silicon carbide supersmooth mirror at 660 nm, and (right) repeatability of this measurement. The pseudocolor height scale is from 5 to -5 nm for both.

The measurement precision is limited by the repeatability between consecutive measurements. The point-by-point difference of 2 consecutive single measurements yields 0.394 nm Sa (Figure 4 (right)), while the point-by-point difference of 2 measurements each consisting of an average of 10 measurements is 0.121 nm Sa. By comparison, commercially available optical profilers usually quote a single measurement repeatability between 0.2-1 nm Sa. When averaging a large number of datasets, commercial profiles quote repeatabilities as low as 0.01 nm Sa in a stable controlled environment.

Measurement precision at the equivalent wavelength scales with the wavelength, and is limited by the noise floor and the repeatability at the single wavelengths. A noise floor of 1 nm at 660 nm becomes 6 nm at the equivalent wavelength of 3.887 µm, while a repeatability of 0.4 nm Sa becomes 2.4 nm Sa at 3.887 µm. Our measurements are consistent with this scaling as long as the wavelength is stable.

### 3.2 Step height standards

VLSI step height standards with calibrated step heights of 182 +/- 2 nm and 952 +/- 6 nm were used to test the multiple wavelength technique. The 182 nm step was measurable at 795 nm, but not at 660 nm, and the 952 nm step was not measurable at either wavelength because this step is higher than a quarter wavelength at each of the measurement wavelengths. Figure 5 shows results of measuring these steps. The surface height maps are shown on the left. Red (center strip, lighter gray) is high and blue (outer rectangles, darker gray) is low. The fields of view are about 450 µm square and the steps are 100 µm wide. Edges were blocked with an analysis mask to bring out the two peaks in the histogram. The 182 nm step looks noisy because it is less than 1/20$^{th}$ of the equivalent wavelength and it also had some debris on it. The 952 nm step is near to a quarter wave of the equivalent wavelength and is very close to the maximum step height that can be measured at this equivalent wavelength. Step heights were determined by finding the distance between peaks of the height histograms on the right. Calculations are done in waves of height where one wave is the equivalent wavelength of 3.887 µm. For the 182 nm step we measured a height of 178.3 nm and for the 952 nm step we measured a height of 952.8 nm. These heights are close to the calibrated step heights, and variations of about +/- 2-3% were seen over multiple repeated measurements.

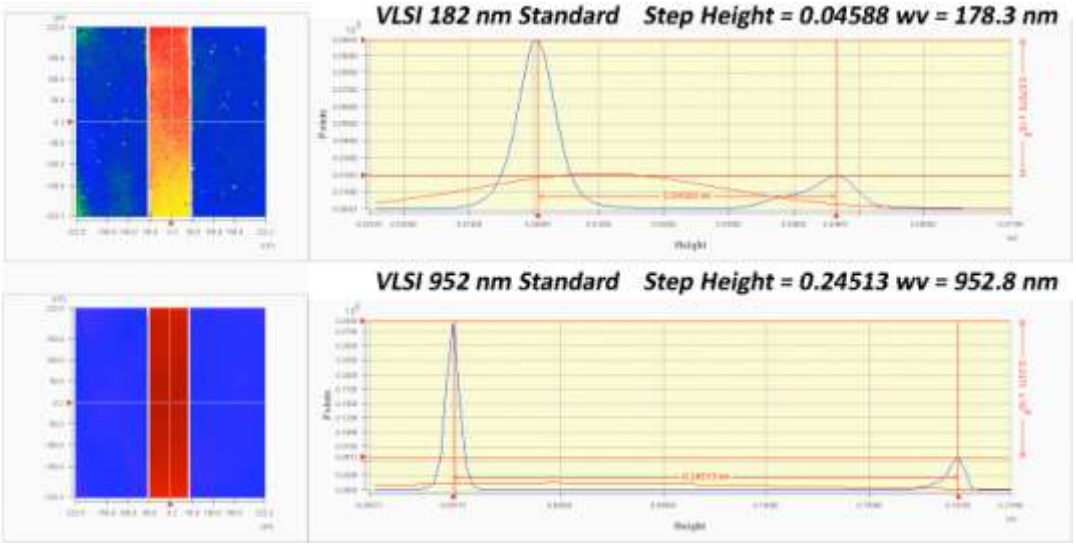


Figure 5. Measurements of VLSI step height standards using multiple wavelength technique.

### 3.3 Roughness comparator gauge

An uncertified GAR S-22 microfinish comparator gauge made by GAR Electroforming for machined surfaces was used to see the range of roughness that could be measured with this breadboard. This gauge is comprised of a series of lapped and ground surfaces with different roughness in terms of microinches of Ra (or Sa). This gauge is used both as a visual aid and as a stylus standard in the machine tool industry. The 8G surface in Figure 6 is ground to have a roughness of 8 µin or 200 nm Ra (or Sa). At a single wavelength (left) not much detail is present and phase unwrapping keeps the profile within +/- 1 wave (660 nm) of height range. When measurements at two wavelengths are combined, the roughness is now 206.8 nm Sa, which is near the nominal value of 200 nm and the vertical range is now over 2 µm. Notice that there is much more detail evident in the multiple wavelength measurement.

Measurements of the GAR 16G gauge surface taken with our breadboard system and compared to a measurement on a Wyko NT-2000 are shown in Figure 7. This surface should be 16 µin or 400 nm Sa. Our measurement on the left has 417.9 nm Sa and shows a lot of details in the grooves. The modulation threshold was set at 2%. The Wyko measurement on the right taken using VSI (vertical scanning interferometry) at 25X with a field of view of ~250 x 185 µm does not show as much detail and has more data dropout. The modulation threshold for the Wyko was set at 4%. When this threshold was lowered for the Wyko system there were unwrap

errors. Neither Wyko instrument we had access to was able to provide as detailed data and had higher dropout rates than our breadboard. These measurements show close to the same spot on the gauge and cover the same area with close to the same resolution and sampling interval. The agreement looks good, and we feel our measurement more closely resembles the actual surface structural detail. The Wyko measurement requires vibration isolation and takes about 5-10 seconds to get all the data. The 4D measurement is acquired in milliseconds without the need for vibration isolation.

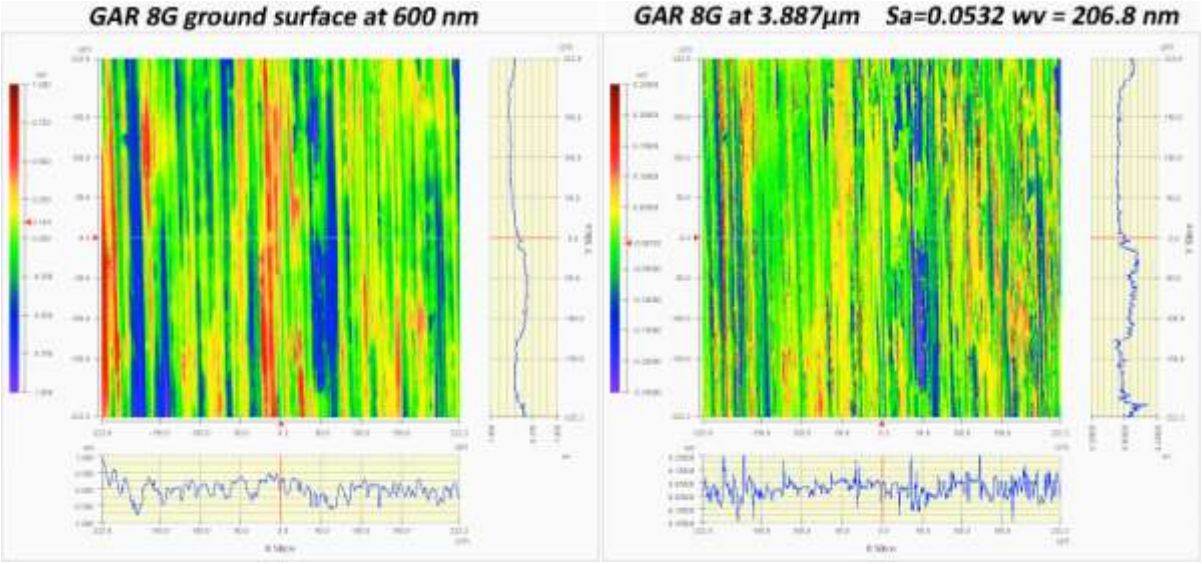


Figure 6. Measurements of GAR 8G microfinish comparator gauge.

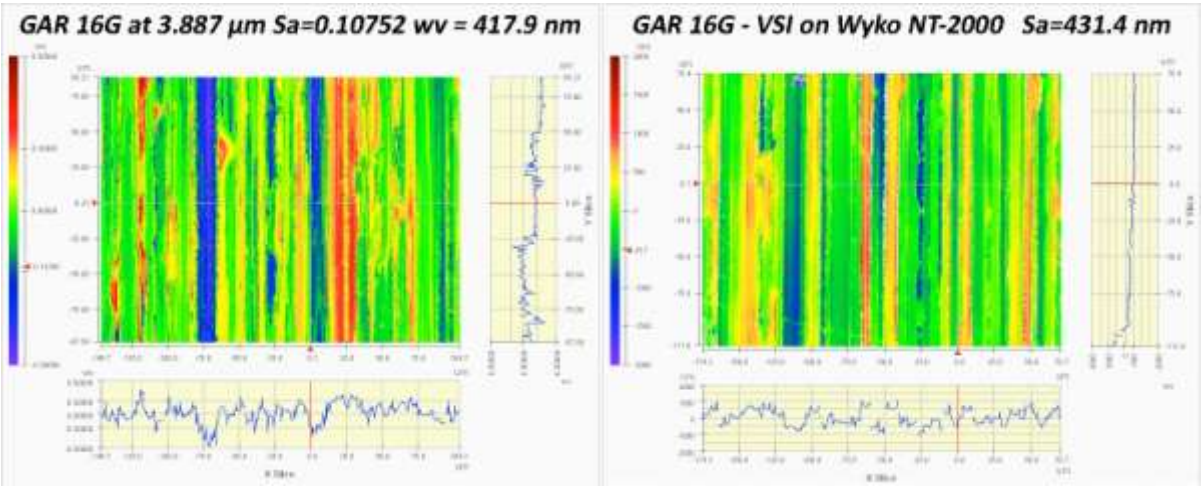


Figure 7. Measurement of GAR 16G surface with multiple wavelengths compared to Wyko VSI.

### 3.4 Bare glass during polishing

To examine bare glass surfaces during different phases of polishing, we obtained a sample from the University of Arizona College of Optical Sciences. This 4" glass wafer was rough ground with a fine grinding grit, and then polished using a slightly curved lap so that the center of the wafer ended up completely polished while at the edge the surface was finely ground. Measurement areas were delineated and numbered across the surface using a black marker so that measurement areas could be consistent within a millimeter or two.

Figure 8 shows measurements at location 17 (about ¾ of the way to the edge) on the sample for the 4D multiple wavelength measurement as well as for a Wyko VSI measurement. Both plots show the same 250 x 185 µm field of view and are located within about 2 mm of one another on the sample. Notice that they both show similar arrangements of pits and polished areas. Because of the large spatial frequency range of this surface, the higher reading from the 4D measurement is most likely due to picking up more detail on the surface, although local variations in the surface could also account for this difference.

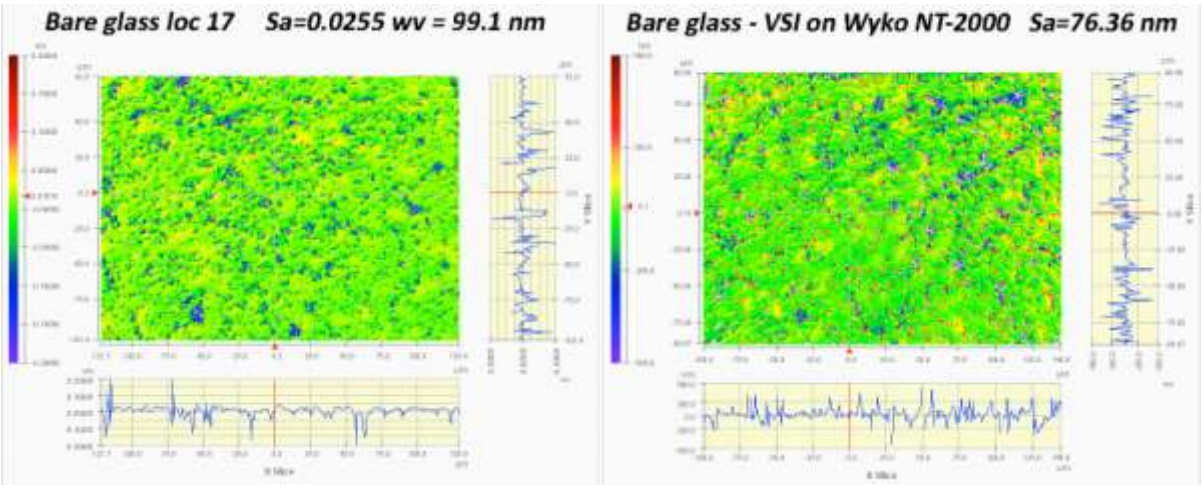


Figure 8. Partially polished bare glass measured with multiple wavelengths compared to Wyko.

Measurements of other areas are shown in Figure 9. Location 16 (left) is more polished than location 17 shown above. Sleeks and pits are easily visible, as is debris piled up around the edges of these features (red areas). At a single wavelength the measured depth of the pits is shallower than they actually are. Multiple wavelengths are necessary to study the depths and the density of the pits and quantify them. Location 18 (right) is near the edge of the sample where the bare glass surface is fine ground with very little polish. The multiple wavelength measurement shows a very rough surface with 251.9 nm Sa. The signal level is good for this measurement and there is little data dropout. We are able to adjust the balance of the test and reference beams by rotating the polarizer in the illumination arm of the microscope, enabling good fringe contrast over a large range of surface reflectivities. These examples show that we are able to measure bare glass surfaces in various states of polish from a fine ground down to a completely polished surface.

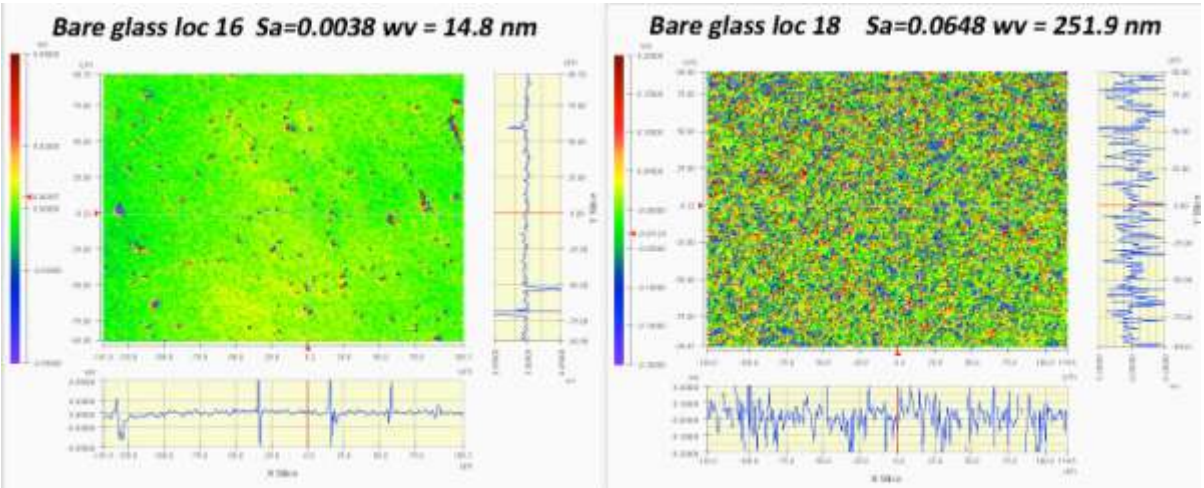


Figure 9. Measurements of partially polished bare glass and fine ground bare glass.

### 3.5 Roughened silicon wafer

A 4” silicon wafer was mounted on a 4” glass wafer and roughened up using a fine grinding compound and then partly polished out leaving a surface with lots of scratch features. Figure 10 shows multiple wavelength measurements at 2 locations on the surface. Note the detail of scratches and pits.

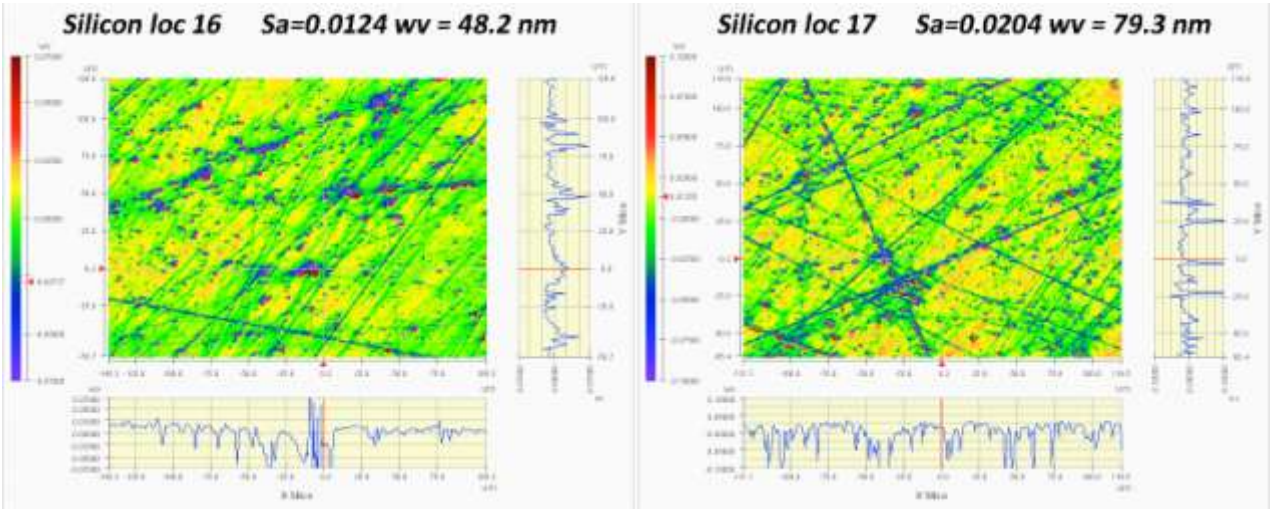


Figure 10. Measurements of roughened then partially polished silicon wafer.

### 3.6 MEMS digital mirror device

To further show the versatility of this technique, we measured a MEMS (micro-electro mechanical system) digital mirror device (DMD) for a digital light projector (DLP) made by Texas Instruments. This device has a glass window over the mirrors to protect them. Most commercial optical profilers are not able to measure through the window because of dispersion induced coherence losses. Our technique using short temporal coherence diode lasers and variable path matching of the Linnik reference arm enable this technique to easily measure this type of object. Addition of the multiple wavelength technique enables more complex objects with depths greater than a quarter of a wavelength to be measured quickly in manufacturing environments.

To better resolve the individual mirrors, the tube lens was replaced with a doublet that increased the field of view by 1.6X yielding a total of 32X with the 20X Linnik. The 795 nm source was replaced with a 687 nm source. When combined with the 660 nm source, this yielded an equivalent wavelength of 16.721 µm. With the two wavelengths this close together, the chromatic aberration was not noticeable. Figure 11 shows two different fields of view that show the mirrors. The center-to-center spacing of the mirrors is 13.6 µm and the height from the top of the mirror to the structure below between the mirrors is about 1 µm. This technique is easily able to resolve details in the mirror array structure. Although a shorter equivalent wavelength would help reduce the measurement noise, these measurements show that we are able to get enough detail to measure critical dimensions.

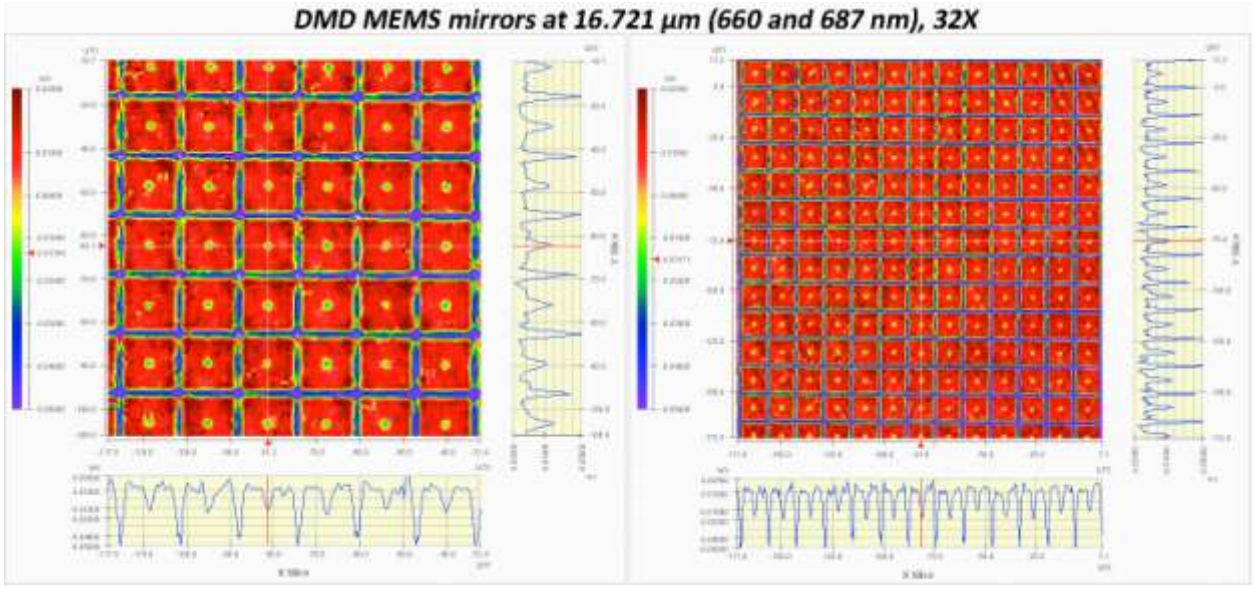


Figure 11. Measurement of mirrors in DMD MEMS device.

## 4. DISCUSSION AND CONCLUSIONS

We have demonstrated "proof of principle" for this novel measurement technology. Measurements from our breadboard system demonstrated the desired vertical range, resolution, and vibration immunity that were the primary goals of this research. We compared our results with a commercial optical profilometer system and believe that our breadboard measurements show better accuracy and spatial resolution, while at the same time were made in the presence of significant vibration.

The breadboard system was limited by the chromatic aberration present in an off-the-shelf microscope tube lens that was used. By designing a lens to compensate for chromatic aberration the image quality should be of high enough quality to implement a multiple wavelength technique across a relatively large wavelength separation of up to 150 nm.

The demonstrated noise floor was near 1 nm Sa ($\lambda$/500) and the single exposure repeatability was <0.4 nm Sa ($\lambda$/1500) at 660 nm. The multiple wavelength performance is on the same order in terms of fractions of the equivalent wavelength. Measurement consistency is currently limited by the wavelength drift of about 3% that we observed. Performance in terms of repeatability of step heights or surface roughness is in the +/-2% range. This is limited mainly by the wavelength drift and slight variations in focus.

This approach is a viable solution for roughness measurement in-situ during manufacturing of bare glass, metal or semiconductor surfaces at various states of fine grinding and polishing. Applications for this technology include flat panel displays, semiconductors, and MEMS as well as measurements through glass windows and critical dimensions of complex and extended objects such as the mirrors in a DMD MEMS device used in DLP (digital light projector) and spacer posts on flat panel display glass.

## 5. ACKNOWLEDGEMENTS

The author would like to thank James Johnson of the College of Optical Sciences, University of Arizona for preparing the bare glass and roughened silicon wafer samples. This work was partially supported by NSF (IIP-1014221).

## 6. REFERENCES


[1] Novak, E., "Microscopy: Interference Microscopy," in [*Encyclopedia of Modern Optics*], Guenther, R. D., Steel, D. G., and Bayvel, L., eds., Marcel Dekker, Amsterdam, 1-9, (2005).

[2] Schmit, J., "Interferometry: White Light Interferometry," in [*Encyclopedia of Modern Optics*], Guenther, R. D., Steel, D. G., and Bayvel, L., eds., Marcel Dekker, Amsterdam, 375-387, (2005).

[3] Schmit, J., Creath, K., and Wyant, J. C., "Chapter 15: Surface Profiling, Multiple Wavelength and White Light Interferometry," in [*Optical Shop Testing, 3rd Edition*], Malacara, D., ed., Wiley, Hoboken, NJ, 667-755, (2007).

[4] Sommargren, G. E., "Optical Heterodyne Profilometry," Applied Optics **20**, 610-618 (1981).

[5] Wyant, J. C., Koliopoulos, C. L., Bhushan, B., and George, O. E., "An optical profilometer for surface characterization of magnetic media," ASLE Trans. **27**, 101-113 (1984).

[6] Schmit, J., Creath, K., and Wyant, J. C., "Ch. 15. Surface Profilers, Multiple Wavelength, and White Light Intereferometry," in [*Optical shop testing; 3rd Edition*], Malacara, D., ed., Wiley-Interscience, Hoboken, N.J., 667-755, (2007).

[7] Abdulhalim, I., "Competence between spatial and temporal coherence in full field optical coherence tomography and intererence microscopy," J Opt A: Pure Appl. Opt. **8**, 952-958 (2006).

[8] Ryabukho, V., and Lyakin, D., "Longitudinal pure spatial coherence of a light field with wide frequency and angular spectra," Optics Letters **30**(3), 224-226 (2005).

[9] Brock, N. J., Millerd, J. E., Wyant, J. C., and Hayes, J. B., "Pixelated phase-mask interferometer ", USPTO, ed., 4D Technology Corporation, United States, (2007).

[10] Kimbrough, B. T., "Pixelated mask spatial carrier phase shifting interferometry algorithms and associated errors," Applied Optics **45**(19), 4554-4562 (2006).

[11] Novak, M., Millerd, J., Brock, N., North-Morris, M., Hayes, J., and Wyant, J., "Analysis of a micropolarizer array-based simultaneous phase-shifting interferometer," Applied Optics **44**(32), 6861-6868 (2005).

[12] Kothiyal, M. P., and Delisle, C., "Shearing interferomter for phase-shifiting interferometry with polarization phase-shifter," Applied Optics **24**(24), 4439-4442 (1985).

[13] Creath, K., "Phase-measurement interferometry techniques," in [*Progress in Optics*], Wolf, E., ed., Elsevier Science Publishers, Amsterdam, 349-393, (1988).

[14] Robinson, D. W., "Phase unwrapping methods," in [*Interferogram Analysis*], Robinson, D. W., and Reid, G. T., eds., IOP Publishing, Bristol, 194-229, (1993).

[15] Blateyron, F., "New 3D Parameters and Filtration Techniques for Surface Metrology," Quality Magazine, 1-7 (2006).

[16] ISO, "ISO/FDIS 25178-2: Geometrical product specifications (GPS) -- Surface texture: Areal -- Part 2: Terms, definitions and surface texture parameters," ISO, (2010).